International Journal of
INTELLIGENT SYSTEMS AND APPLICATIONS IN ENGINEERING
ISSN:2147-6799 www.ijisae.org Original Research Paper

Solar PV Based EV Charging using Moth-Flame Optimization (MFO) Algorithm Based ANFIS Energy Management System

[1]Bandana Gautam, [2]Rajnish Bhasker

Submitted: 07/02/2024 **Revised**: 15/03/2024 **Accepted**: 21/03/2024

Abstract: This paper provides a new energy management method for electric vehicle charging in ANFIS based Moth flame optimization (ANFIS-MFO) for the Energy management. The proposed system consists of a grid connected Solar PV system & battery powered energy management system, which is a combination of solar PV and battery power. The system is based on a moth flame algorithm tuned ANFIS technique is used to find optimal power reference for the EV battery based on SOC of the battery. In the proposed system, the peak power of the solar PV system is captured and analyzed. The performance of the proposed method tested with standard P&O-MPPT method. The effective execution of the suggested operation for each mode occurred, and a reduction in the cost of power purchase from the grid was achieved through the proposed MFO EMS. Additionally, the charging and discharging of the battery were carried out effectively without any loss. The simulation is carried out in MATLAB/SIMULINK and the outputs are validated.

Keywords: *Pv, EV, ANFIS, Moth flame optimization*

I. INTRODUCTION

As the world faces a critical situation with the decline of fossil fuels and the harmful effects of global warming, there has been a surge in popularity for another energy sources. Among these renewable resources such as hydel, wind, tidal, and solar energy has emerged as the greatest favored option due to its ability to convert energy without emitting pollutants. Over the last 15 years, the need for solar power has increased from 25% to 30%. One of the many merits of solar power is its eco-friendliness and abundance in nature. The management of this energy system heavily relies on power electronics [1-2]. The DC power generated by a PV source can be converted into AC power by utilizing a Power Electronics converter. This converted energy can then be utilized to power local loads or supplied to the grid for broader use. Numerous sources suggest the importance of this converter in enabling the proper functioning of the solar energy system [3-5].

PV cells typically have a low conversion efficiency, with a voltage range of approximately 0.5-0.8V. Monitoring the maximum power point of the PV system is imperative for optimizing performance. Inclusion of a battery is necessary to ensure a consistent power supply to the load, given the intermittent nature of the PV energy source. This battery can store excess energy for later use or supply the energy to the local load or grid as needed. For a dependable and regular power supply, it is important to include a battery in a solar energy system, according to many sources [6-7]. The balance relating the energy provided and the energy used by the load determines the mode of operation for a solar energy system. This balance can vary based on different operating modes. By utilizing a bi-directional converter, it is possible to reduce the number of batteries needed for energy storage while making sure that electricity stays on even in the event that one of the cells fails. This converter offers several advantages and is a recommended component for a well-functioning solar energy system [8] A comprehensive survey of the MFO algorithm was published in [9], covering its development from inception to April 2019. The authors provided a detailed analysis of various MFO method alternatives, including any improvements, modifications, or hybridizations that have been made. Furthermore, they examined the diverse range of fields where the MFO algorithm was utilized in the following field i.e., engineering, medical, and machine learning. This survey paper serves as a valuable resource for those interested in the MFO algorithm and its various applications. A literature study on the MFO algorithm was published in [10], covering all the variants of the algorithm This study analyses improvements, binary and multi-objective versions, hybridizations, modifications, and applications in the fields of engineering, chemistry, medicine, machine learning, fuzzy logic, image segmentation, networking, etc., along with information on the relevant journals and publishers., fuzzy inference systems (FIS), neuro-fuzzy systems and Artificial neural networks (ANN) are examples of intelligent control strategies that have become more and more popular in recent years for industrial automation. These schemes operate without requiring a same model of the system and are immune to system subtleties, making them advantageous in most of the nonlinear systems [11-12]. ANFIS is one of the neuro-fuzzy models that is thought to be simpler, quicker, more accurate, and stronger in generalisation

[1]*M.tech student,Department of Electrical Engineering UNSIET, VBS PURVANCHALUNIVERSITY JAUNPUR,222003*
[2]*Professor & Head, Department of Electrical Engineering UNSIET VBS PURVANCHAL UNIVERSITY JAUNPUR,*

abilities [13]. In order to mimic the cognitive powers of the human mind, it inherits the learning and parallel data processing abilities of artificial neural networks as well as the inference capability of fuzzy inference systems.

II. PROPOSED SYSTEM

The Proposed structure Block Diagram is depicted in Figure.1. Here the system comprises of a PV & battery as a Input source it is linked to the AC Grid via a Inverter.

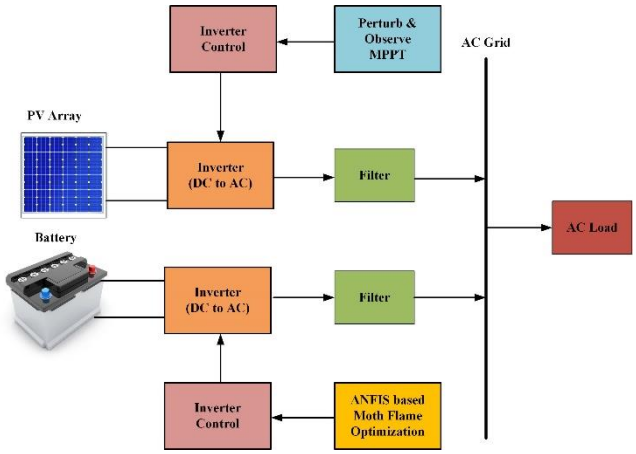

Fig.1 Overall Operation Block of ANFIS-MFO EMS System

A. Solar PV system

Figure 2 represents an analogous circuit model for the PV cell, which is utilized to calculate the photovoltaic reference model output current (IPV) based on the output voltage (VPV), as well as the cell temperature (TC) and irradiance (G). The output power, current, and voltage of the solar PV reference model are significantly influenced by these parameters. Equations (1) and (2) are used to determine the connection between PV current and voltage.

$$I_{PV} = I_{SC} \times \left[1 - A_1 \times \left(e^{\left(\frac{V_{PV}}{A_2 \times V_{OC}}\right)} - 1\right)\right] \quad (1)$$

Equation 1, also referred to as the I-V equation, is used to show how the output voltage (V_{PV}) and current (I_{PV}) of a photovoltaic cell correlate at various light levels. This equation is widely employed to describe the characteristics of PV cells.

Where,

$$A_1 = \left(1 - \frac{I_{MP}}{I_{SC}}\right) \times e^{\left(\frac{-V_{MP}}{A_2 \times V_{OC}}\right)}$$
$$A_2 = \frac{\left(\frac{V_{MP}}{V_{OC}} - 1\right)}{\ln\left(1 - \frac{I_{MP}}{I_{SC}}\right)} \quad (2)$$

Where,

The A1 parameter in the equation is influenced by the features of a photovoltaic cell, and its value decreases as IMP / ISC increases and with increasing VMP, as described in the equation. A2 is another parameter that governs how quickly A1 diminishes with increasing VMP. MPP corresponds to the point at which the solar PV module generates the maximum power, denoted by IMP. ISC represents the current obtained by the solar PV array when no voltage is applied to it. VMP refers to the voltage at MPP, while VOC is the voltage generated by the PV cell or module when the current through it is zero.

Various factors, such as temperature and irradiance, impact the VMP, IMP, VOC, and ISC parameters of a PV panel. The relationship between these parameters and the current-voltage (I-V) plot of a PV module can be described by equations (3), (4), and (5), which take into account of the of temperature (TC) and irradiance (G).

$$I_{SC}(G, T_C) = I_{SCS} \times \frac{G}{G_S} \times \left(1 + \delta \times (T_C - T_S)\right)$$
$$I_{MP}(G, T_C) = I_{MPS} \times \frac{G}{G_S} \times \left(1 + \delta \times (T_C - T_S)\right) \quad (3)$$

Parameters such as temperature and solar intensity influence current of a photovoltaic unit at the short-circuit, represented as I_{SC} (Tc, G). At typical test circumstances with a cell temperature of approximately 25°C and an air mass of 1.5, the short-circuit current is identified as I_{SC}. The reference intensity equal to 1000 W/m2 (Gs), and the temperature constant of short-circuit current, alpha (indicating the degree of current decrease with temperature increase), are integral to this relationship. T_S (25°C) represents the reference temperature. The current at the maximum power point (MPP) generated by the PV unit under precise temperature and intensity circumstances is I_{MP} (Tc, G), with IMPS representing the MPP current during STC. Equation (3) establishes the relationship between I_{SC} and I_{MP} with G and T_C, incorporating the parameters and their dependencies.

$$V_{OC}(T_C) = V_{OCS} + \varepsilon \times (T_C - T_S)$$
$$V_{MP}(T_C) = V_{MPS} + \varepsilon \times (T_C - T_S) \quad (4)$$

$V_{OC(T\,C)}$ = PV unit's open-circuit voltage for specified temperature.

$V_{OCS=}$ The OC voltage during STC

ε = A measure of how much the voltage changes with temperature is the OC voltage's temperature constant.

V_{MPS}= The voltage at MPP when STC .

Equation (4) links V_{OC} and V_{MP} to T_C by using the previously mentioned factors and their interdependencies.

$$T_C = 1.14 \times (T - T_S) + 0.0175 \times (G - 300) \quad (5)$$

The photovoltaic (PV) module's thermal behavior is modeled using an equation that relates the module temperature (T), cell temperature (TC), and irradiance (G). The Standard temperature is 25°C. The Cell temperature and the irradiance are dependent on the module temperature. These equations take into consideration the influence of temperature coefficients and other parameters on the I-V characteristics of the PV unit under different temperature and irradiance circumstances and are thus regarded to be exact representations.

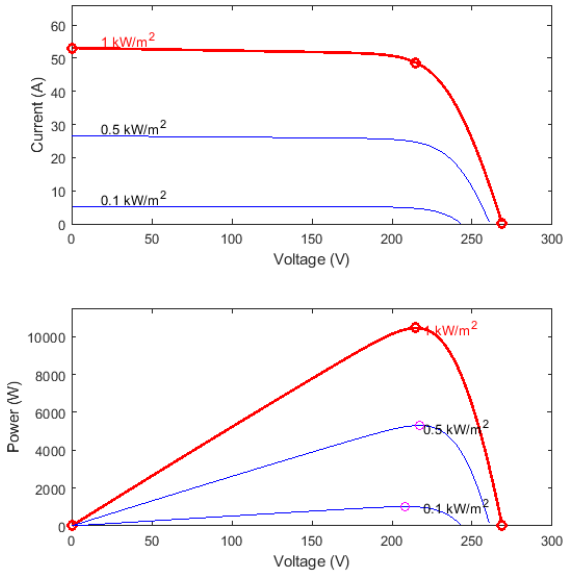

Fig.2. IV and PV characteristics of the considered PV array

B. Perturb & Observe MPPT

The effectiveness of PV array is highly dependent on their efficiency in generating energy. Because of the extremely nonlinear power characteristics of solar cells, external variables like irradiance & temperature continually affect how much energy they can produce. Monitoring solar cell output voltage constantly is essential to maximizing energy production and ensuring that it stays nearby to the extreme power point despite temperature and irradiance changes. Its total efficiency is increased by monitoring and collecting the solar PV system's peak output continually throughout the day, which ultimately boosts the productivity of the solar cell. With every release, MPPT algorithms gain traction and become more efficient.

The MPPT regulator may use a variety of MPPT approaches, including perturbation and observation (P&O) , Incremental conductance (IC) and fuzzy logic controller. The selection of an algorithm depends on various factors such as the design requirements of the system, including its speed, complexity, and reliability. To identify and obtain peak power from solar PV systems, two MPPT algorithms were developed in this study: P&O MPPT and fuzzy MPPT. Because of its low rate and simplicity of connection, the perturbation and observation (P&O) approach has grown acceptance in solar photovoltaic systems. To calculate the PV power, this method measures the voltage and current data from the PV module. Equation (6) is used to guide algorithmic changes as well as boost converter modifications based on the comparative findings.

$$D_{k+1} = D_k \pm \Delta D \quad (6)$$

The P&O MPPT method follows a particular process to determine the ideal duty cycle. Every cycle, the perturbations that have come before and since, Dk and Dk+1, are added together with a step size D, resulting in Dk+1 + Dk. The PV current and voltage are measured, and power, instantaneous change in current, previous instant power (P), and instantaneous change in voltage (V) are calculated. If Power is superior than zero, the procedure checks V. D decreases the duty cycle if V is likewise bigger than zero and increases it otherwise. D increases the duty cycle if P is less than 0 and V is larger than 0; if not, D decreases the duty cycle. An overview of the MPPT algorithm procedure for perturbation and observation is shown in Table 1.

Table 1. PO Perturbation Probability

ΔP	ΔV	D
+	+	+
+	-	-
-	+	-
-	-	+

Three major obstacles must be overcome by the P&O MPPT system: a protracted convergence time; variations in the vicinity of the peak power point; and a drifting problem brought on by abrupt changes in irradiance and partial shade situations. In the PO MPPT system, the magnitude of the step size ΔD is important since a big variation in decay time might result in rapid settling and severe fluctuations. while a small ΔD results in smoother oscillations and a slower steady-state. The key feature of the MPPT procedure is the determination of the direction of the Perturb and Observe (PO) MPPT algorithm, dictating how it tracks steady state peak power point. Yet, this change in track only happens with an upsurge in intensity, leading to a decrease in the efficiency of the PO MPPT. The proposed adaptive PO MPPT method with a adjustable step size to address these problems was discussed by researchers, but it is still regarded as an insufficient solution. Potential solutions to overcome the limitations of the standard Perturbation and Observation MPPT method have been suggested in the form of soft calculation techniques based on PV peak power point trailing methods. A summary of the route of the Perturbation and Observation MPPT procedure is provided in Table 1.

C. DC–AC converter

An inverter control system is responsible for converting DC electricity to AC power and reducing high-frequency harmonics in the grid system using an AC filter. The parameter control method is used by the controller to generate PWM logic signals for the inverter's switches. The main parts of the inverter are the IGBT and filters, while the DC connector and filtering circuitry are auxiliary components. Stabilizing the input voltage from the DC power supply to the inverter system involves the utilization of a 600 uF capacitor. Connection to the grid is established through an AC filter, aiming to mitigate the influence of harmonics originating from the grid. The voltage control loop and the inner current loop, constituting the regulator system, are overseen by a PI controller. An increase in electrical dependability is achieved by ensuring that the VSI inverter is operated with a certain amount of energy to stabilise the DC link voltage Vdc.

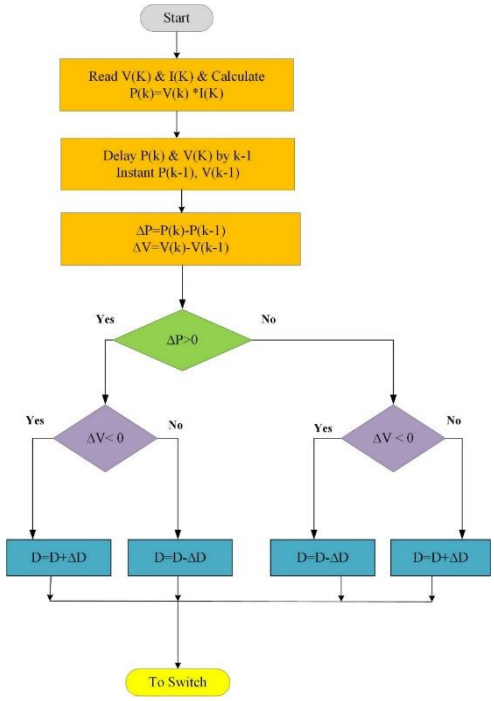

Fig 3. Flowchart of Perturb & Observe MPPT

III. ADAPTIVE NEURO FUZZY INFERENCE SYSTEM

Figure 8 depicts the ANFIS architecture, which comprises five levels. Unlike fuzzy c-mean, scatter partition, and tiered separation, the grid partition procedure divides the input space into subsets that are likely to include input vectors, bringing the number of rules down to a manageable amount.. Layer 1, also called as the input fuzzification layer, is where input is fuzzified. This layer uses a mathematical expression, provided by the equation, to assign membership values to each subset of the given input space in the fuzzy system.

$$o_{ij}^{(1)} = \mu_j(I_{ij}^{(1)}) \tag{7}$$

The second tier of the ANFIS design is called the Fuzzy AND operation layer, Here, the T-norm operator of the algebraic product is used by each node to conduct a fuzzy-AND operation. The result of each node is its output, which is its product.

$$o_k^{(2)} = \omega_k = \prod_{i=1}^{q} o_{ij}^{(1)} \tag{8}$$

The third layer of the ANFIS architecture is called the normalizing layer. Its purpose is to compute the outcome of every node by dividing the activation value of each rule in the fuzzy system by the total amount of all the initial values. This step normalizes the initial values of the fuzzy rules to ensure that they all contribute to the final output proportionally.

$$o_k^{(3)} = \overline{\omega_k} = \frac{o_k^{(2)}}{\sum_{m=1}^{y^2} o_m^{(2)}} \tag{9}$$

Nodes with linear factors make up the fourth layer of the ANFIS architecture. Every node k in this layer implements the direct function, which is represented by an equation, and has a set of corresponding variable parameters (d1k, d2k,... dyk, d0).

$$o_k^{(4)} = \overline{\omega_k}\, f_k = \overline{\omega_k}\,(d_{1k} I_1^{(1)} + d_{2k} I_2^{(1)} + \cdots + d_{yk} I_y^{(1)} + d_0) \tag{10}$$

The fifth layer in the ANFIS model includes a single node that produces the network's output by algebraically summing up all the inputs. Horse Herd Optimization is used for optimizing the ANFIS parameters; the specifics of this procedure are covered in the section that follows..

$$U_a = o^5 = \sum_{k=1}^{y^2} o_k^{(4)} = \sum_{k=1}^{y^2} \overline{\omega_k} f_k = \frac{\sum_{k=1}^{y^2} \omega_k f_k}{\sum_{k=1}^{y^2} \omega_k} \tag{11}$$

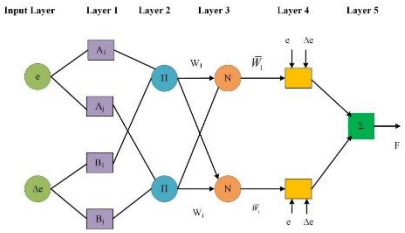

Fig 4. Layers of ANFIS Network

There are several methods for determining the mean squared error (MSE).

$$MSE = \left(\frac{1}{N}\right) \sum_i |t_i - o_i|^2 \tag{12}$$

The ANFIS network's tunable parameters are adjusted using the PSO technique in an effort to minimize the mean squared error—that is, the difference among the target value (t) and the yield value (o). N is the total amount of outputs in the output layer of the network.

IV. MOTH FLAME OPTIMIZATION ALGORITHM

This section provides information on the MFO methods history and its functioning procedure with scientific formulations in Sections A and B, respectively.

A. Inspiration

Moths are an insect species belonging to the class Arthropoda. They feature two sets of large arms coated in scales, a thorax, two antennae, a head, six legs, and an abdomen.. They are nocturnal creatures that rely on moonlight for navigation, and their unique navigation techniques have captured the interest of metaheuristics researchers. According to Fig. 3, moths navigate by using an oblique orientation mechanism. Moths maintain a steady angle with the moon, resulting in a crosswise leaning, to keep their journey straight. As the distance from a flame decreases, a helical route signal is initiated to link the moth with the flare, ensuring effective steering. Moths employ distance from a flame to help in their navigation.

MFO Algorithm

Each location in basic MFO is described as a matrix of decision factors, and each moth represents a possible resolution.

$$X = \begin{bmatrix} X_1 \\ X_2 \\ : \\ : \\ X_N \end{bmatrix} = \begin{bmatrix} x_{1,1} & x_{1,2} & \cdots & x_{1,n-1} & x_{1,n} \\ x_{2,1} & \ddots & \cdots & \cdots & x_{2,n} \\ \vdots & \cdots & \ddots & \vdots & \vdots \\ x_{N-1,1} & \cdots & \cdots & \ddots & x_{N-1,n} \\ x_{N,1} & x_{N,2} & \cdots & x_{N,n-1} & x_{N,n} \end{bmatrix}$$

where i = 1, 2,..., N, and Xi = xi,1, xi,2,..., xi,n.The problem's dimension is represented by the number n, where n is the numeral of moths. An illustration of a moth's fitness is displayed as a vector below:

$$Fit[X] = \begin{bmatrix} Fit[X_1] \\ Fit[X_2] \\ : \\ : \\ Fit[X_n] \end{bmatrix}$$

Below is a display of the flame matrix. Since every moth flies around a flame, the size must match that of the moth matrix previously described.

$$FM = \begin{bmatrix} FM_1 \\ FM_2 \\ : \\ : \\ FM_N \end{bmatrix}$$

$$= \begin{bmatrix} Fm_{1,1} & Fm_{1,2} & \cdots & Fm_{1,n-1} & Fm_{1,n} \\ Fm_{2,1} & \ddots & \cdots & \cdots & Fm_{2,n} \\ \vdots & \cdots & \ddots & \vdots & \vdots \\ Fm_{N-1,1} & \cdots & \cdots & \ddots & Fm_{N-1,n} \\ Fm_{N,1} & Fm_{N,2} & \cdots & Fm_{N,n-1} & Fm_{N,n} \end{bmatrix}$$

The flame matrix's matching fitness is shown below.

$$Fit[FM] = \begin{bmatrix} Fit[FM_1] \\ Fit[FM_2] \\ : \\ : \\ Fit[FM_n] \end{bmatrix}$$

The moth and the flame are the two main characters of MFO. In order to get the desired effects, the moth must pass through the flame. The following equation defines the logarithmic twisting function, which is useful to simulate the moth's twisting motion:

$$X_i^{K+1} = \begin{cases} \delta_i . e^{bt} . \cos(2\pi t) + Fm_i(k), i \le N.FM \\ \delta_i . e^{bt} . \cos(2\pi t) + Fm_{N.FM}(k), i \ge N.FM \end{cases}$$

The formula _i = XKi Fmi shows the separation between a moth at point Xi and its consistent flare (Fmi). The twisting aeronautical search is resolute by b and t (a arbitrary numeral among -1 and 1), which indicate how accurate the moth is approaching its flame in Fig. 4. A moth is seen flying in a helix pattern towards a similar flame in Fig. 5. The cost of t falls across the repetitions, matching the examination and manipulation at the start and end of the repetitions. Fig. 6 displays the moth's next position along with a mathematical illustration of it.

$$r = -1 + Current_{\ iter} \left(\frac{-1}{Max_{iter}} \right)$$

$$t = (r - 1) \times k + 1$$

When Max_{iter} is the Extreme number of repetitions, k is a random integer between 0 and 1, and r is the convergence-ensuring constant, whose value decreases, Every iteration, the flame location for the previous and current repetitions is gathered and sorted based on the universal and limited search fitness values. Only the finest N.FM blazes are kept, while other fires are extinguished, resulting in the one flaw that was briefly mentioned. The finest and worst fitness levels are the first and last flames, respectively. The moths then arrived in the same sequence to snare each flame individually. Over the course of the number of repetitions, the similar- and low-level moths will always catch the final flame. The MFO algorithm's operational flow is shown in Figure 7 for twenty starting moths across 500 iterations (the representation of MO and FM in Fig. 7 stand for moth and flame, respectively). The quantity of flames (N.FM) that have been lowered during the repetition may be calculated using the formula below.

$$N.FM = round \left(N.FM_{Lastiter} - Current_{iter} \frac{(N.FM_{Lastiter} - 1)}{Max_{iter}} \right)$$

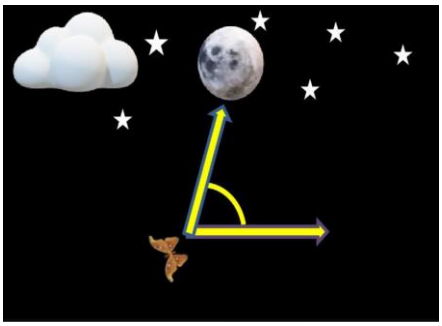

Figure 5. A moth's nighttime flight path

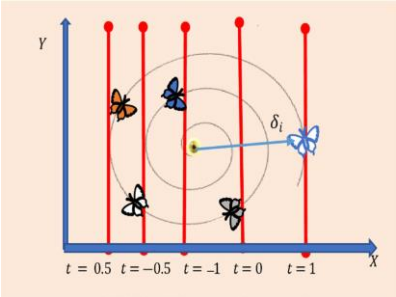

Fig 6. Spiral of a logarithm in relation to time

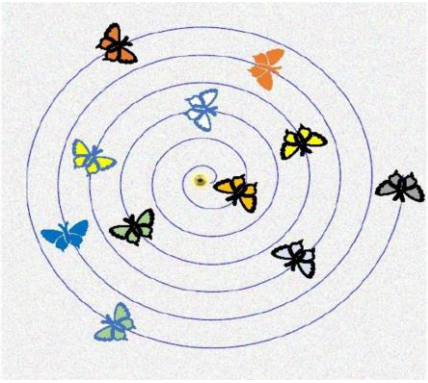

Fig 7. Moth turning in a spiral around the flame

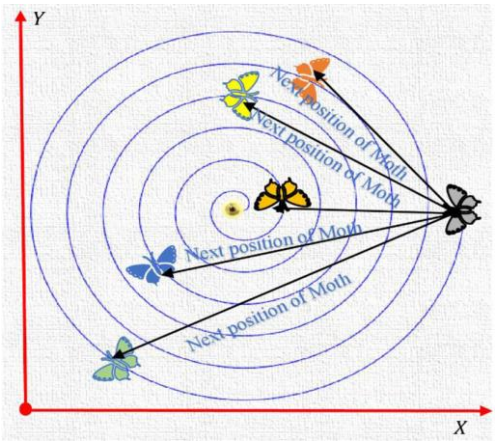

Fig 7. Place of Moth

V. SIMULATION RESULTS & DISCUSSIONS

MATLAB/Simulink software is used to construct and evaluate the simulation model of the solar PV-based EV charging utilizing the Moth-flame Optimization (MFO) Method based ANFIS energy control system. The proposed system's simulated circuit diagram is shown in Figure 8.

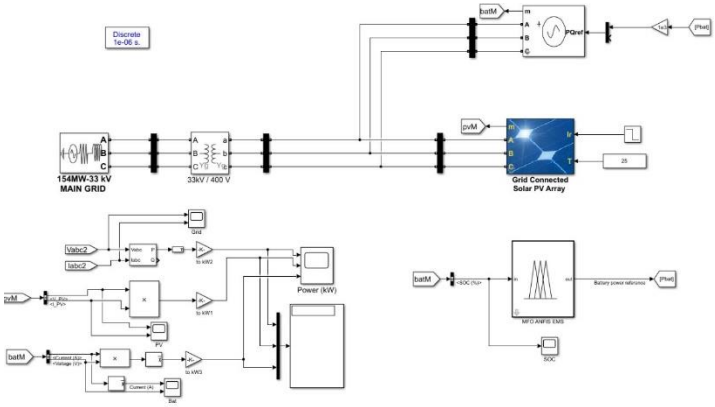

Fig 8 Simulation Circuit Diagram

Figure 9 & 10 shows the moth flame convergence plot and the training diagram of the ANFIS with moth flame optimization is represented. SOC of the battery and power reference are considered as input and output for the ANFIS controller for training. The moth flame reach the global minimum point at 25 iteration with root mean square error of the training process.

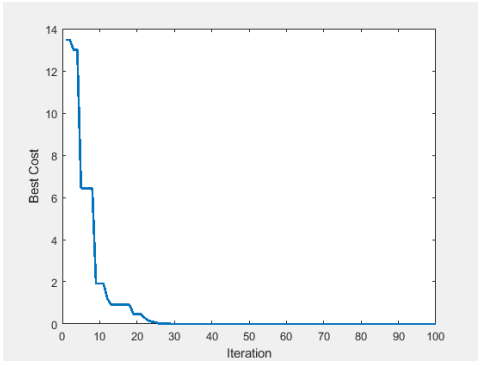

Figure 9. Moth flame convergence graph

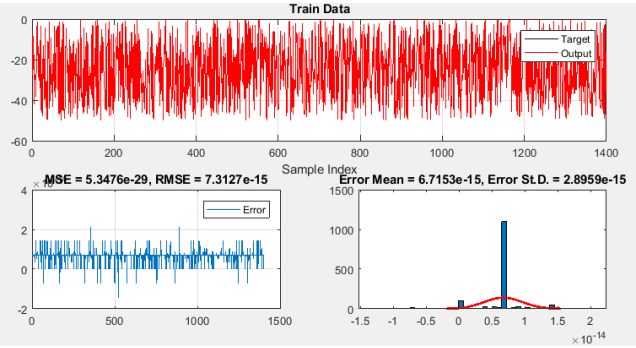

Fig 10. Training of ANFIS with MFO

Figures 11 and 12 display the Solar PV scheme voltage and current. PV irradiation ranges from 1000 to 500 w/m2 for 0.5 seconds. At 1000 irradiance, the PV current and voltage are 600A and 510 V, respectively. At 500 irradiances, the PV current and voltage are 300 and 508A, respectively.

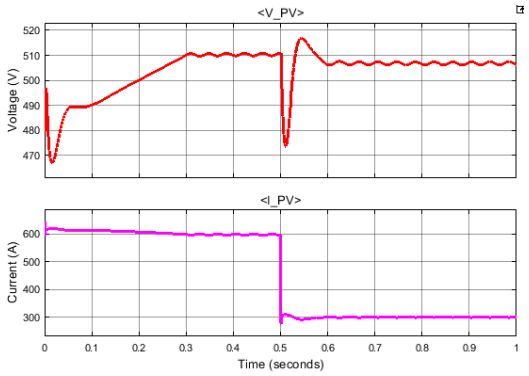

Fig 11. PV Voltage and Current

Figure 12 shows the EV Battery Current and Voltage. The SOC of the battery is depicted in figure 13. The EV Battery voltage is maintained at 510 V and current is keep increase from 0 seconds and after 0.5 seconds EV battery current is maintained at 65 A. The SOC of the EV battery is increases from 25 % to 25.004 % from 0 to 1 seconds.

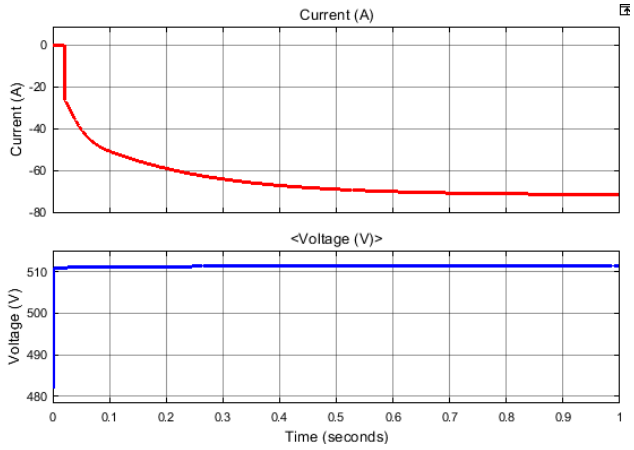

Fig 12. Battery current and voltage

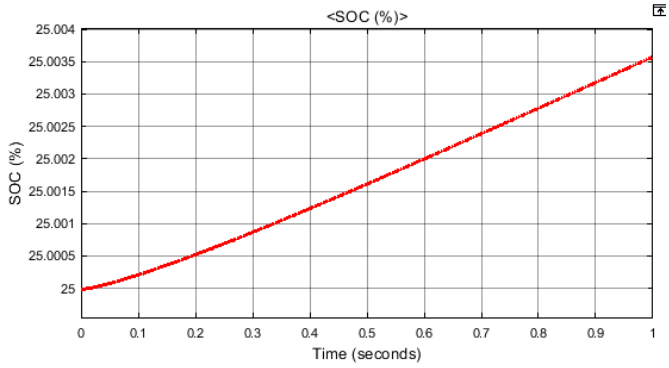

Fig 13 SOC of the Battery

Figure 14 displays the Grid's voltage and current. Grid current is kept at 150 A, while grid voltage is kept at 230 V rms.

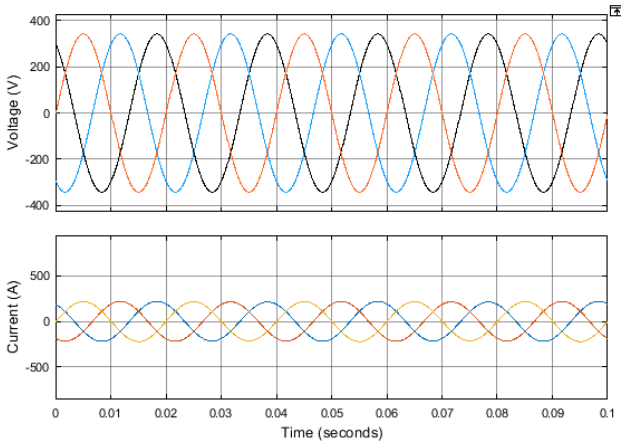

Fig 14. Grid Voltage and current

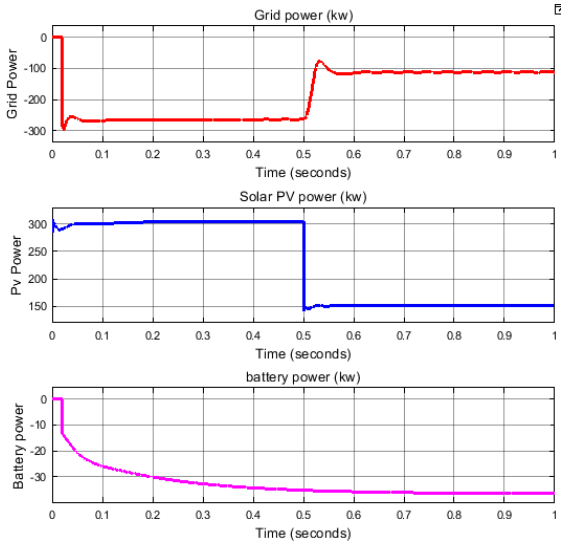

Fig 16. Power of grid, PV and battery

Figure 16 depicts the grid, photovoltaic, and battery power. The PV electricity is utilized for charging the EV battery for 0 to 0.5 seconds, with any surplus power being sent to the grid. From 0.5 to 1 seconds, PV power decreases to 150 kW and grid power reduces to 100 kw. Here EV battery power maintained constant power charging of 38 kw. From these test results, MFO optimized ANFIS energy management effectively control the battery charging without any delay and loss.

V. CONCLUSION

The paper suggests a novel method for energy management that is based on ANFIS-trained moth flame optimization. Here the PV & battery are connected to the grid. PV is employed with Perturb & observe MPPT & Inverter control. Here the SOC of the battery is monitored consistently according to the change in the SOC of the battery the Charging & Discharging of the Energy management is done. As the Electric vehicle battery is charged & discharged effectively. Better control of energy among the source and the grid, as well as for charging EV batteries, is provided by the suggested system with ANFIS-MFO training. Each mode's recommended operation was successfully completed, and the ANFIS moth flame optimization EMS

led to a decrease in the price of grid power procurement. If the ANFIS-MFO based technique is implemented in the stand-alone operation mode, it is envisaged that the EMS operation process may further be improved.

References

[1] S.K. Kim, J.H. Joen, C.H. Cho, J.B. Ahn, and H Kwon, Dynamic modelling and control of a grid-connected hybrid generation system with versatile power transfer, *IEEE Trans. Ind. Electron.*, vol. 55, no. 4, p. 1677-1688, Apr. 2008.

[2] F. Valenciaga and P.F. Puleston, Supervisor control for a stand-alone hybrid generation system using wind and photovoltaic energy, *IEEE Trans. Energy Conv.*, vol. 20(2), p. 398-405, June 2005.

[3] Hamrouni N, Jraidi M, Chérif A. New control strategy for 2-stage grid connected photovoltaic power system. *Renewable Energy*, 2008; 33(10):p. 2212–21.

[4] Barbosa PG, Rolim LGB, Watanabe EH, Hanitsch R. Control strategy for grid connected DC–AC converters with load power factor correction. *IEEE Procedings. Gener, Transm Distrib*, 1998; 145(5): p. 487– 492.

[5] Koutroulis E, Kalaitzakis K, Voulgaris NC., Development of a microcontroller based, photovoltaic maximum power point tracking control system. *IEEE Transactions on Power Electronics*, 2001; 16(1): p. 46–54.

[6] Boucetta Abd Allah, Labed Djamel, Control of Power and Voltage of Solar Grid Connected. *International Journal of Electrical and Computer Engineering (IJECE)*, Vol. 6, No. 1, February 2016, pp. 26~33.

[7]] Use of Photovoltaics in Microgrid as Energy Source and Control Method using MATLAB/Simulink, *International Journal of Electrical and Computer Engineering (IJECE)*, Vol. 6, No. 2, April 2016, pp. 851~858.

[8] http://www.batteryuniversity.com/partone-24.htm

[9] Shehab M, Abualigah L, Al Hamad H, Alabool H, Alshinwan M, Khasawneh AM (2020) Moth–flame optimization algorithm: variantsand applications. Neural Comput Appl 32(14):9859–9884.

[10] Hussien AG, Amin M, Abd El Aziz M (2020) A comprehensive review of moth-flame optimisation: variants, hybrids, and applications. J Exp Theor Artif Intell 32(4):705–725.

[11] Li, H., Shi, K. L., & McLaren, P. G. "Neural-network-based sensorless maximum wind energy capture with compensated power coefficient." IEEE transactions on industry applications 41.6 (2005): 1548-1556.

[12] Jang, J. R. "ANFIS: adaptive-network-based fuzzy inference system." IEEE transactions on systems, man, and cybernetics 23.3 (1993): 665- 685.

[13] García, P., García, C. A., Fernández, L. M., Llorens, F., & Jurado, F. "ANFIS-based control of a grid-connected hybrid system integrating renewable energies, hydrogen and batteries." IEEE Transactions on